Z. Phys. B 94, 91–100 (1994)

ZEITSCHRIFT
FÜR PHYSIK B

Polaron formation and hopping conductivity in the Holstein-Hubbard model

H. Fehske[1], **D. Ihle**[2], **J. Loos**[3], **U. Trapper**[2], **H. Büttner**[1]

[1] Physikalisches Institut, Universität Bayreuth, D-95440 Bayreuth, Germany
[2] Fachbereich Physik, Universität Leipzig, D-04109 Leipzig, Germany
[3] Institute of Physics, Czech Academy of Sciences, 16200 Prague, Czech Republic

Received: 14 October 1993

Abstract. On the basis of the Holstein-Hubbard model the formation of polarons at finite densities is investigated by means of a variational approach appropriate for describing squeezing and correlation effects. An effective Hubbard model for the polarons is derived, where the correlations are treated within the slave-boson saddle-point approximation. For low enough phonon frequencies, with increasing coupling an abrupt self-trapping transition from light to heavy polarons is found. With increasing density the squeezing effect increases, and the transition is shifted to higher couplings. In the case of an effective Coulomb repulsion, the self-trapping transition is shifted to lower couplings with increasing Hubbard interaction, and the effective polaron mass below the transition is enhanced. In the heavy polaron regime, the frequency-dependent polaron hopping conductivity is calculated. There occur qualitative finite-density and correlation effects on the zero-temperature absorption spectrum which are discussed with respect to their possible relevance to the midinfrared absorption in high-T_c superconductors.

PACS: 63.20.Kr; 71.38.+i; 72.90.+y

1. Introduction

The formation of tight-binding polarons in strongly coupled electron-phonon systems is a problem of current interest [1–8]. Recently, it was suggested that polaron formation may also play an important role in high-T_c superconductors [9], e.g., for the explanation of the anomalous midinfrared optical absorption in the insulating and metallic phases [10–12].

One of the basic problems in this field is the sharp transition from quasi-free electrons to self-trapped heavy polarons with increasing coupling strength [2–4, 6, 8]. All the previous theories concerned with this problem adopt the single-polaron picture which is only justified in the limit of very low carrier densities (realized, e.g., in photoinduced absorption). Thereby, the spinless Holstein model [1] (describing a short-range electron-phonon interaction) was treated by variational [2, 4] and Monte Carlo methods [6]. On the basis of this model, Toyozawa [2] has found, at low enough phonon frequencies, a discontinuous self-trapping transition. The previous theories of polaron transport are also based on the single-polaron picture [1, 4, 5, 13–16].

The study of finite-density effects on the polaron formation and transport is of particular importance. For instance, in the high-T_c materials, the density of charge carriers introduced by doping can be varied continuously and may have appreciable values. Attempts at taking into consideration finite densities in the polaron formation were made by Feinberg et al. [17]. Those authors, using a variational approach and including squeezing effects, have obtained an abrupt self-trapping transition in the spinless model at half-filling. However, the density dependence of this transition was not yet studied. Moreover, until now there is no theory of polaron formation (self-trapping transition) in the Holstein-Hubbard model for spin-$\frac{1}{2}$ electrons at finite densities, where correlation effects become important. Recently, Suzuki et al. [18] have taken into account arbitrary densities in the theory of polaron conductivity on the basis of the Holstein-Hubbard model using the "normal" Lang-Firsov transformation [5].

In our previous paper [19], we have analyzed the main features of the ground-state phase diagram of the Holstein-Hubbard model by means of a variational slave boson theory. This approach, based on a modified variational Lang-Firsov transformation, facilitates a unique treatment of electron-electron and electron-phonon interaction, and allows an interpolation between weak and strong coupling regimes as well as between adiabatic and antiadiabatic limits. However, to discuss the interplay of dimerization and polaronic effects near half-filling, in [19], we have limited ourselves to the case of moderate electron-phonon coupling, i.e. weak mass renormalization.

In this paper we focus our attention to the case, where due to strong electron-phonon coupling a substantial mass renormalization of the quasiparticles may take place (heavy polarons). Our aim is to investigate, for the first time, the polaron formation in the Holstein-Hubbard model at *finite* densities. Along this line, we analyze the squeezing and correlation effects on the self-trapping transition over a wide range of model parameters. We also study the polaron formation in the spinless fermion model. For comparison with the variational method used by Feinberg et al. [17], we apply two different versions of our variational procedure which are critically analyzed throughout the paper. Then, in a next step, we calculate the polaron hopping conductivity, discuss the correlation and finite-density effects in the heavy polaron regime, and compare our results with those by Suzuki et al. [18].

The paper is organized as follows. In Sect. 2 we present our variational approach to the Holstein-Hubbard model. Performing two types of unitary polaron transformations and a squeezing transformation, we derive, in the ground state of the transformed phonon vacuum, an effective polaronic Hubbard Hamiltonian. In Sect. 3 we treat the polaron formation (in particular the self-trapping transition) in the Hartree-Fock approximation and for the spinless Holstein model. In Sect. 4 we study the correlation effects within the slave-boson approach. In Sect. 5 we calculate the polaron hopping conductivity to lowest order in the polaronic reduced transfer integral, where we focus on the zero-temperature absorption spectrum. The conclusions of our investigations can be found in Sect. 6.

2. Model and variational approach

We consider a system of correlated electrons locally coupled to a dispersionless optical mode with frequency ω_0, described by the Holstein-Hubbard model

$$\mathscr{H} = -t \sum_{\langle i,j\rangle\sigma} c_{i\sigma}^{\dagger} c_{j\sigma} + U \sum_i n_{i\uparrow} n_{i\downarrow} - g\hbar\omega_0 \sum_{i,\sigma} (b_i^{\dagger} + b_i) n_{i\sigma} + \hbar\omega_0 \sum_i (b_i^{\dagger} b_i + \tfrac{1}{2}). \tag{1}$$

The exact relation $\langle [b_i, \mathscr{H}]_- \rangle_{\mathscr{H}} = 0$ ($\langle \ldots \rangle_{\mathscr{H}}$ is the thermal average with respect to $\mathscr{H}$) yields the mean shift in the equilibrium positions of the local oscillators given by $\langle b_i \rangle_{\mathscr{H}} = g \langle n_i \rangle_{\mathscr{H}}$, where $n_i = \sum_\sigma n_{i\sigma}$. We restrict ourselves to the non-dimerized paramagnetic phase, i.e. we adopt $\langle n_i \rangle_{\mathscr{H}} = n$. This is correct far enough from half-filling [19].

We treat the formation of polarons and the squeezing phenomena (in terms of two-phonon coherent states) by a variational approach [17, 19–21]. As a first step, we perform the unitary transformation

$$|\Psi\rangle = \mathscr{U} |\tilde{\Psi}\rangle, \quad \tilde{\mathscr{H}} = \mathscr{U}^{\dagger} \mathscr{H} \mathscr{U}, \quad \mathscr{U} = \prod_{i=1}^{2} e^{-S_i}, \tag{2}$$

where $|\Psi\rangle$ and $|\tilde{\Psi}\rangle$ denote the eigenstates of $\mathscr{H}$ and $\tilde{\mathscr{H}}$, respectively, and $\mathscr{U}$ contains different variational parameters.

To describe the polaron formation at finite densities, we use a modified variational Lang-Firsov transformation (MVLF) given by

$$S_1(\bar{\gamma}, \gamma) = -g \sum_i (b_i^{\dagger} - b_i)(\bar{\gamma} + \gamma n_i). \tag{3}$$

The parameter $\bar{\gamma}$ may be obtained from $\langle \tilde{b}_i \rangle_{\tilde{\mathscr{H}}} = \langle b_i \rangle_{\mathscr{H}} = g n$ ($\tilde{b}_i = \mathscr{U}^{\dagger} b_i \mathscr{U}$) with $\langle b_i \rangle_{\tilde{\mathscr{H}}} = 0$ or by minimisation of the ground-state energy with respect to $\bar{\gamma}$. We get $\bar{\gamma} = n - \gamma n$, where the first term takes into consideration the mean oscillator shift and the second term describes the polaronic lattice distortion in S_1 due to the density fluctuation $n_i - n$. Note that our approach generalizes that by Zheng et al. [21] to arbitrary band fillings. Since Feinberg et al. [17] have used, for finite densities, the variational Lang-Firsov transformation (VLF) given by (3) with $\bar{\gamma} \equiv 0$, we also consider the VLF in comparison with the MVLF. Note that for $\bar{\gamma} \equiv 0$ and $\gamma \equiv 1$, S_1 becomes the "normal" Lang-Firsov transformation (LF) [5].

To describe squeezing effects, which become relevant at finite polaron densities, after S_1 we perform the squeezing transformation [17, 20, 21]

$$S_2(\alpha) = -\alpha \sum_i (b_i^{\dagger} b_i^{\dagger} - b_i b_i) \tag{4}$$

generating two-phonon coherent states. By (1) to (4) we obtain

$$\begin{aligned} \tilde{\mathscr{H}} = & -\tilde{\varepsilon}_p \sum_i n_i + \tilde{U} \sum_i n_{i\uparrow} n_{i\downarrow} - t \sum_{\langle i,j\rangle\sigma} \tilde{\Phi}_{ij} c_{i\sigma}^{\dagger} c_{j\sigma} \\ & + g\hbar\omega_0 \tau^{-1} \sum_i (b_i^{\dagger} + b_i)[(\gamma - 1) n_i + \bar{\gamma}] + \bar{\gamma}^2 \varepsilon_p N \\ & + \hbar\omega_0 \sum_i \{ \tfrac{1}{2}(\tau^2 + \tau^{-2})(b_i^{\dagger} b_i + \tfrac{1}{2}) \\ & - \tfrac{1}{4}(\tau^2 - \tau^{-2})(b_i^{\dagger} b_i^{\dagger} + b_i b_i) \}, \end{aligned} \tag{5}$$

where

$$\tilde{\varepsilon}_p = \varepsilon_p [\gamma(2 - \gamma) + 2(1 - \gamma)\bar{\gamma}], \tag{6}$$

$$\tilde{U} = U - 2\varepsilon_p \gamma(2 - \gamma), \tag{7}$$

$$\tilde{\Phi}_{ij} = \exp\{-g\gamma\tau(b_i^{\dagger} - b_i - b_j^{\dagger} + b_j)\}, \tag{8}$$

$$\varepsilon_p = g^2 \hbar\omega_0, \quad \tau = e^{-2\alpha}. \tag{9}$$

For $\bar{\gamma} \equiv 0$, $\gamma \equiv 1$ and $\tau \equiv 1$, $\tilde{\mathscr{H}}$ becomes the well-known small-polaron Hamiltonian [5], where ε_p denotes the small-polaron binding energy in the $t = 0$ limit.

As the next step in our variational approach to the polaron formation at $T = 0$, the ground state of $\mathscr{H}$ is approximated by the variational state $|\Psi_V\rangle = \mathscr{U} |\tilde{\Psi}_V\rangle$ taking the ansatz

$$|\tilde{\Psi}_V\rangle = |\tilde{\Psi}_p\rangle \otimes |\tilde{\Psi}_e\rangle. \tag{10}$$

Equation (10) corresponds to the decoupling of the transformed phonon and electron subsystems described

by $\tilde{\mathscr{H}}$. From (5) to (10) we obtain the effective polaronic Hamiltonian $\mathscr{H}_{\text{eff}} \equiv \langle \tilde{\Psi}_p^0 | \tilde{\mathscr{H}} | \tilde{\Psi}_p^0 \rangle$, where $|\tilde{\Psi}_p^0\rangle$ is the transformed phonon vacuum, given by

$$\mathscr{H}_{\text{eff}} = \sum_{\mathbf{k},\sigma} (\rho\, \varepsilon_{\mathbf{k}} - \tilde{\varepsilon}_p)\, c_{\mathbf{k}\sigma}^{\dagger} c_{\mathbf{k}\sigma} + \tilde{U} \sum_i n_{i\uparrow} n_{i\downarrow} + \left(\bar{\gamma}^2 \varepsilon_p + \frac{\hbar\omega_0}{4} (\tau^2 + \tau^{-2}) \right) N. \tag{11}$$

Here,

$$\rho = \exp\{-\varepsilon_p \gamma^2 \tau^2 / \hbar\omega_0\} \tag{12}$$

is the polaronic band narrowing factor, and $\varepsilon_{\mathbf{k}} = -2t \sum_{i=1}^{D} \cos(k_i a)$ (D is the dimensionality). Finally, the variational parameters (γ, τ^2) are determined by minimisation of the ground-state energy $\langle \tilde{\Psi}_e | \mathscr{H}_{\text{eff}} | \tilde{\Psi}_e \rangle$.

To separate the polaron correlation effects due to $\tilde{U}$ (combined Coulomb repulsion and phonon-induced attraction), we first consider two versions of $\mathscr{H}_{\text{eff}}$ describing uncorrelated polarons.

3. Uncorrelated polarons

To study the finite-density and squeezing effects on the polaron formation, we take the spin-$\frac{1}{2}$ ($s=\frac{1}{2}$) model (11) in the Hartree-Fock approximation. For comparison, we also consider the spinless ($s=0$) Holstein model resulting in the effective Hamiltonian of the form (11) without spin sum and interaction term.

To simplify the analytical calculations, in this section we express the **k**-summation in terms of the square density of states. Measuring, hereafter, all energies in units of t, we obtain the ground-state energy per site ($s=\frac{1}{2}, 0$)

$$f(\bar{\gamma}, \gamma, \tau^2) = \bar{\gamma}^2 \varepsilon_p - n \left\{ \tilde{\varepsilon}_p + 4\rho \left(1 - \frac{n}{2s+1} \right) \right\} + s \frac{n^2}{2} \tilde{U} + \frac{\hbar\omega_0}{4} (\tau^2 + \tau^{-2}). \tag{13}$$

In addition, we have

$$\bar{\gamma} = \begin{cases} (1-\gamma)n, & \text{MVLF} \\ 0, & \text{VLF}. \end{cases} \tag{14}$$

Minimizing f, the variational parameters γ and τ^2 are determined from the equations

$$\gamma = \hbar\omega_0 \{\hbar\omega_0 + \varepsilon_{c_1} \rho\, \tau^2\}^{-1}, \tag{15}$$

$$\tau^2 = \hbar\omega_0 \{(\hbar\omega_0)^2 + \varepsilon_p \rho\, \gamma^2\, \varepsilon_{c_1}^2 / \varepsilon_{c_2}\}^{-1/2}, \tag{16}$$

where

$$\varepsilon_{c_1} = \begin{cases} 4, & \text{MVLF} \\ 4\,\dfrac{2s+1-n}{2s+1+2sn}, & \text{VLF}, \end{cases} \tag{17}$$

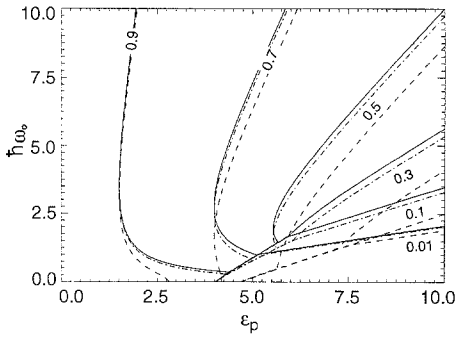

Fig. 1. Contourplots of the polaronic band narrowing factor ρ in the $\hbar\omega_0 - \varepsilon_p$ plane for the uncorrelated $s=\frac{1}{2}$ case using the MVLF. Solid curves show the results without squeezing ($\tau^2 \equiv 1$), which are independent of the polaron density n. Chain dotted (short-dashed) curves correspond to the case $\tau^2 \neq 1$ for $n=0.1$ ($n=0.7$)

and

$$\varepsilon_{c_2} = \varepsilon_{c_1}^2 \left\{ 16\, n \left(1 - \frac{n}{2s+1} \right) \right\}^{-1}. \tag{18}$$

In the variational analysis, the solution of the extremal equations (15) and (16) must be used to find the absolute minimum of the ground-state energies for both the MVLF and the VLF.

We characterize the polarons by their effective mass expressed in terms of the band narrowing factor, $m^*/m = \rho^{-1}$, as function of the model parameters ε_p and $\hbar\omega_0$ and of the polaron density n. For a detailed classification within different $\hbar\omega_0 - \varepsilon_p$ regimes we refer to [17]. We also do not investigate the spatial extent of the polarons in the weak and strong-coupling regimes. In the strong-coupling case ($\varepsilon_p \gg 1$), for small polarons we have $\rho \ll 1$.

Solving the variational equations (13) to (18), some results are shown in Fig. 1 as constant-ρ contours in the $\hbar\omega_0 - \varepsilon_p$ plane for different n. We have compared the results including squeezing with those neglecting squeezing ($\tau^2 \equiv 1$). For all $\hbar\omega_0$, ε_p and n we have found

$$f_{\text{MVLF}} < f_{\text{VLF}} < f_{\text{LF}}, \tag{19}$$

where, in each case, the energy is lowered by the inclusion of the squeezing effect. Neglecting squeezing effects, the ρ-contours for the MVLF are identical in the Hartree-Fock solution and the spinless model and do not depend on n.

Next we consider the adiabatic limit ($\omega_0 \to 0$). By (12) and a low-frequency expansion, we obtain three solutions of (15) and (16),

$$\text{I:}\ \gamma = \frac{\tau^{-2}}{\varepsilon_{c_1}} \hbar\omega_0, \qquad \tau^2 = \left(1 - \frac{\varepsilon_p}{\varepsilon_{c_2}} \right)^{\frac{1}{2}};$$

$$\text{II:}\ \gamma = 1, \qquad \tau^2 = 1;$$

$$\text{III:}\ \gamma = 1 - \left(\frac{\varepsilon_{c_2}}{\varepsilon_p} \rho \right)^{\frac{1}{2}}, \qquad \tau^2 = \frac{1-\gamma}{\varepsilon_{c_1} \gamma} \hbar\omega_0. \tag{20}$$

At $\omega_0 = 0$, we have $\rho = 1$ for solution I and $\rho = 0$ for solution II. For solution III, we get the relation

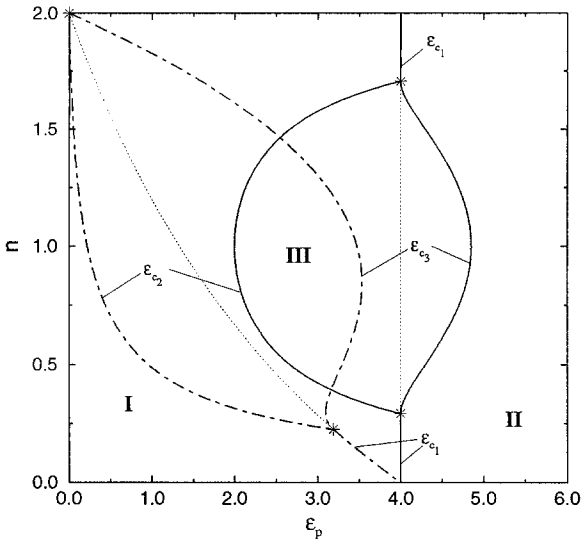

Fig. 2. Stability regions I, II and III of the corresponding ($s=\frac{1}{2}$) Hartree-Fock solutions (20) in the adiabatic limit. The solic (chain dashed) curves denote the boundaries for the MVLF (VLF), where ε_{c_1}, ε_{c_2} and ε_{c_3} are given by (17), (18) and (22), respectively. The symbol (*) marks the triple point. Dotted curves indicate the transition line I$\rightleftharpoons$II neglecting the squeezing effect ($\tau^2 \equiv 1$)

$$\varepsilon_p = \varepsilon_{c_2}\rho\left(\frac{\varepsilon_{c_1}}{\varepsilon_{c_2}}\ln\rho - 1\right)^2. \tag{21}$$

Let us point out that solution III, where $\tau^2 \to 0$ ($\alpha \to \infty$) as $\omega_0 \to 0$, yields a finite zero-point energy of phonons and a vanishing variance of the ion coordinates within the uncertainty principle in its minimal form [17].

Analyzing the stability of the *paramagnetic* solutions (20) by comparing the corresponding ground-state energies (13), we obtain the stability regions in the $n-\varepsilon_p$ plane shown in Fig. 2. Of course, near half-filling ($0.7 \lesssim n \lesssim 1.3$) symmetry-broken solutions (e.g. charge or spin ordered states) may have a lower free energy, as shown in our previous work [22, 23].

For $n<n_c$ ($\varepsilon_{c_2}>\varepsilon_{c_1}$), where n_c is determined from $\varepsilon_{c_2}=\varepsilon_{c_1}$, with increasing ε_p we get an abrupt transition from the free electron state I to the perfectly localised self-trapped state II at the critical coupling ε_{c_1}. Such a discontinuous change in the effective mass at the self-trapping transition, well-known in single-electron theories [2, 3, 8], was also found by Feinberg et al. [17] (for $\omega_0>0$) in the spinless half-filled band model applying the VLF. Let us stress that we get $f_{\mathrm{MVLF}}<f_{\mathrm{VLF}}$, i.e., the MVLF treats the finite-density problem more correctly. Whereas in the MVLF the transition point does not depend on n ($\varepsilon_{c_1}=4$), the VLF yields a decrease of ε_{c_1} with increasing n (in the limit $n=0$ we have $\varepsilon_{c_1}=4$ in all cases).

For $n>n_c$ ($\varepsilon_{c_2}<\varepsilon_{c_1}$), with increasing ε_p we obtain a continuous transition from I to III at ε_{c_2} and a discontinuous self-trapping transition from III to II at ε_{c_3} (see Fig. 2), where

$$\varepsilon_{c_3} = \frac{\varepsilon_{c_1}^2}{\varepsilon_{c_2}}\rho_{c_3}, \qquad \rho_{c_3} = \exp\left\{-\left(1-\frac{\varepsilon_{c_2}}{\varepsilon_{c_1}}\right)\right\}, \tag{22}$$

and in the region $\varepsilon_{c_2}<\varepsilon_p<\varepsilon_{c_3}$ the band narrowing factor decreases from $\rho=1$ to $\rho=\rho_{c_3}$. Note that the two successive transitions do not occur in the spinless model treated by the MVLF, since $\varepsilon_{c_2}<\varepsilon_{c_1}$ cannot be fulfilled. The occurrence of the triple point ($\varepsilon_{c_1}=\varepsilon_{c_2}=\varepsilon_{c_3}$) is a finite density effect realized via the squeezing effect. Neglecting squeezing ($\tau^2 \equiv 1$) we have no solution III, and only the abrupt self-trapping transition from I to II at ε_{c_1} takes place (indicated, for $n>n_c$, by the dotted lines in Fig. 2). As can be seen from Fig. 1, squeezing increases with increasing n towards half-filling and shifts the self-trapping transition to higher values of ε_p ($\varepsilon_{c_3}>\varepsilon_{c_1}$). Obviously, the best treatment of the polaron formation yields the highest value of the self-trapping transition point.

Considering the finite-frequency range, without squeezing, the sharp transition from light polarons ($\rho \lesssim 1$) to self-trapped heavy polarons ($\rho \ll 1$) takes place at $\varepsilon_{c_1}(\omega_0)$ increasing with ω_0 from ε_{c_1}, given by (17), up to the critical point $\varepsilon_{c_1}(\omega_{c_1})$, whereby the magnitude of the discontinuity in ρ decreases. For $\omega_0>\omega_{c_1}$ the discontinuity disappears, and we get a smooth crossover from light to heavy polarons with increasing ε_p, in qualitative agreement with previous results [2, 3, 17]. The situation is analogous to that in the gas-liquid first-order transition [2], if we let ω_0 correspond to the temperature, ρ to the volume, and ε_p to the pressure. For $\tau^2 \equiv 1$, the critical point may be determined analytically starting from $\varepsilon_p(\rho, \omega_0) = -\ln\rho(\hbar\omega_0 + \varepsilon_{c_1}\rho)^2/\hbar\omega_0$. From the conditions $\partial\varepsilon_p/\partial\rho|_{\rho_{c_1},\omega_{c_1}}=0$ and $\partial^2\varepsilon_p/\partial\rho^2|_{\rho_{c_1},\omega_{c_1}}=0$ we obtain $\rho_{c_1}=\exp(-3/2)$, $\hbar\omega_{c_1}=2\rho_{c_1}\varepsilon_{c_1}$, and $\varepsilon_{c_1}(\omega_{c_1}) = \frac{27}{4}\rho_{c_1}\varepsilon_{c_1}$.

Taking into account squeezing effects, for $n<n_c$ the self-trapping transition point $\varepsilon_{c_1}(\omega_0)$ is shifted to higher values of ε_p, and the critical-point value ω_{c_1} becomes smaller (see Fig. 1). For $n>n_c$ (compare Fig. 2), the abrupt self-trapping transition takes place at $\varepsilon_{c_3}(\omega_0)$ increasing with ω_0 (Fig. 1), except for the spinless model treated by the MVLF. Because $\varepsilon_{c_3}(\omega_0)>\varepsilon_{c_1}(\omega_0)$, squeezing reduces the heavy polaron region.

Finally, let us consider the anti-adiabatic limit ($\omega_0 \to \infty$). Here, we get $\gamma=1$ and $\tau^2=1$ for arbitrary ε_p and n. Note that, although the polaron effect is strongest, according to (12) we have light polarons ($\rho=1$).

4. Correlated polarons

In the Hartree-Fock approximation to the model (11), the polaron formation does not depend on the effective interaction $\tilde{U}$. However, from physical arguments we suggest that a repulsive intrasite interaction $\tilde{U}$ increases the effective polaron mass and favors the self-trapping tendency. In this section, our aim is to investigate the correlation effects on the polaron formation due to the effective Coulomb repulsion $\tilde{U}>0$, where we consider, as in Sect. 3, the homogeneous paraphase which is stable for sufficiently large deviations from half-filling (see the phase diagram in [22, 23]). To this end, we start from the effective Hubbard model (11) and use the slave-boson approach, introduced by Kotliar and Ruckenstein [24], on the level of the paramagnetic saddle-point approxi-

mation. For the Hubbard model in the absence of symmetry-breaking phases, this approximation was shown to be equivalent to the Gutzwiller variational approach [24]. A detailed presentation of the slave-boson saddle-point approximation applied to the Holstein-Hubbard model, including charge-ordered and different magnetically ordered phases, is given in [22, 23] ($\omega_0 = 0$) and in [19] ($\omega_0 > 0$).

We follow the approach indicated in [24, 25] and start from the functional integral representation of the partition function for the model (11) expressed in terms of an effective slave-boson action. Using the saddle-point approximation, all Bose fields (and Lagrange multipliers) are taken to be independent of the site indices and time. The solution of the saddle-point equations (obtained by minimisation of the ground-state energy with respect to the slave-boson variables) yields the ground-state energy per site at the saddle point,

$$f(\bar{\gamma}, \gamma, \tau^2) = \bar{\gamma}^2 \varepsilon_p - n\tilde{\varepsilon}_p + q\rho\bar{\varepsilon} + \tilde{U} d^2 + \frac{\hbar\omega_0}{4}(\tau^2 + \tau^{-2}). \quad (23)$$

Here,

$$\bar{\varepsilon} = \frac{2}{N}\sum_{\mathbf{k}} \varepsilon_{\mathbf{k}}\, \Theta(\varepsilon_F - q\rho\varepsilon_{\mathbf{k}}) \quad (24)$$

(ε_F is the Fermi energy and Θ the step function),

$$q = \frac{2y - y^2 - (1-n)^2}{n(2-n)} \quad (25)$$

is the correlation-induced band narrowing factor for the lower Hubbard subband ($n < 1$),

$$d^2 = \frac{(y+n-1)^2}{4y} \quad (26)$$

is the probability for double site-occupancy, and $y > 0$ is given by the solution of the equation

$$\frac{\tilde{U}}{\rho} = \frac{8\bar{\varepsilon}}{n(2-n)} \frac{y^2(y-1)}{y^2 - (1-n)^2}. \quad (27)$$

Equation (27) takes into account the correlation effects which are determined by the ratio $\tilde{U}/\rho$ (instead of U for the pure Hubbard model). The Fermi energy has to be determined from

$$n = \frac{2}{N}\sum_{\mathbf{k}} \Theta(\varepsilon_F - q\rho\varepsilon_{\mathbf{k}}), \quad (28)$$

where, motivated by the layered structure of the high-T_c superconductors, the exact tight-binding density of states for the square lattice is used. For the Holstein-Hubbard model, in our variational method, the self-consistency equations (27) and (28) must be supplemented by the extremal equations for γ and τ^2 derived from (23). We obtain

$$\gamma = \frac{(n + 2d^2 - \bar{\gamma} n)\hbar\omega_0}{(n+2d^2)\hbar\omega_0 - q\rho\bar{\varepsilon}\tau^2}, \quad (29)$$

$$\tau^2 = \hbar\omega_0 \{(\hbar\omega_0)^2 - 4\varepsilon_p q\rho\bar{\varepsilon}\gamma^2\}^{-\frac{1}{2}}. \quad (30)$$

In the solution of the self-consistency equations (27) to (30) with (24) to (26) for both the MVLF and the VLF, we have to guarantee that $\tilde{U} > 0$ in the whole parameter range of $\hbar\omega_0$, ε_p and n, in particular in the self-trapped heavy polaron region (compare Fig. 1). Therefore, the Hubbard interaction U has to be chosen large enough. The case $\tilde{U} < 0$ may give rise to bipolaron formation.

Let us consider two limiting cases of the ground-state energy (23) using the square density of states which gives $\bar{\varepsilon} = -4n(1-n/2)$. Putting $\tilde{U} \equiv 0$ in (27) ($y = 1$), we get $q = 1$ and $d^2 = n^2/4$ so that (23) becomes the Hartree-Fock result (13). Considering the limit $\tilde{U}/\rho \to \infty$ (the effective interaction $\tilde{U}/\rho$ becomes extremely large in the heavy polaron region), from (26) and (27) we have $\lim_{(\tilde{U}/\rho)\to\infty} \tilde{U} d^2 = 0$. By (27), we get $y = 1 - n$ so that

$$\lim_{(\tilde{U}/\rho)\to\infty} q = \frac{1-n}{1-n/2}. \quad (31)$$

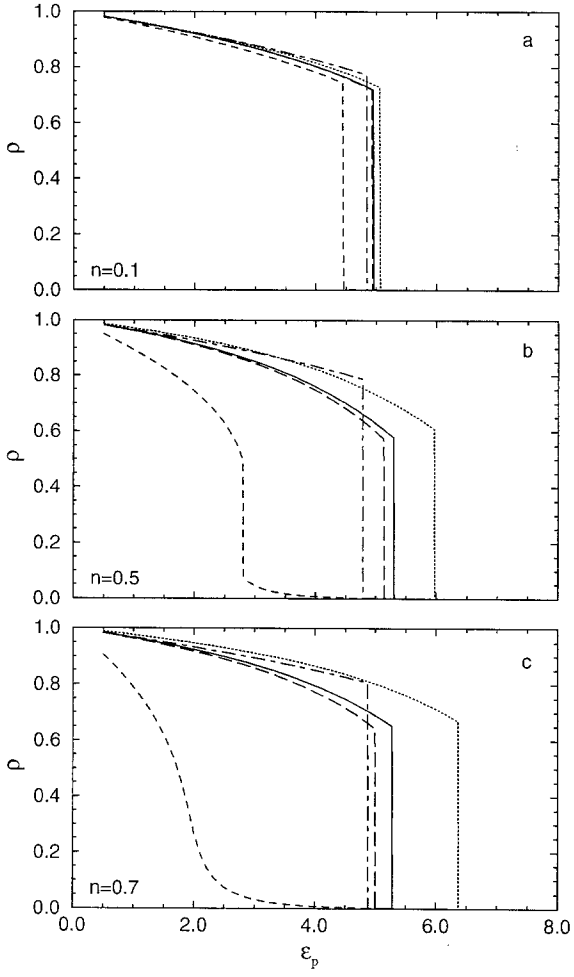

Fig. 3. Polaron band narrowing ρ as function of the polaron binding energy ε_p at $\hbar\omega_0 = 0.8$ for different band-fillings $n = 0.1$ **a**, 0.5 **b** and 0.7 **c**. Solid (long-dashed) curves denote the MVLF results including the squeezing effect at Hubbard interaction $U = 15$ ($U = 20$). The dotted line shows ρ vs ε_p for $U = 15$ using the square density of states. At $U = 15$, results for the MVLF and the VLF without squeezing are given by chain dashed and short-dashed curves, respectively

Using the $\bar{\varepsilon}$ value given above for the square density of states, we obtain $q\bar{\varepsilon} = -4n(1-n)$, and (23) changes to the ground-state energy (13) for the spinless model.

We have solved numerically the coupled system of self-consistency equations (24) to (30), including the determination of the absolute minimum of the ground-state energy (23), and show some representative results in Figs. 3 to 7.

For a fixed frequency ($\hbar\omega_0 = 0.8$), at which the self-trapping transition may occur (see Fig. 1), in Fig. 3 the dependence of the polaron narrowing factor ρ on ε_p, n, and U is illustrated. Note that above the transition point, our approach yields an extremely strong band narrowing ($\rho \lesssim 10^{-3}$). For comparison, the results obtained without squeezing and by means of the square density of states are also depicted. The large difference of the results obtained by the exact and square densities of states may be explained, according to (12), by the exponential dependence of ρ on $\bar{\varepsilon}$. The chosen parameters permit the separation of the correlation effects from the squeezing effects. First, we obtain the result that, at fixed n, with increasing Hubbard interaction U the self-trapping transition is shifted to lower values of ε_p, whereby this effect increases with the polaron density. This is also corroborated by comparing the transition points in the Hartree-Fock approximation and the spinless model (corresponding to the limit $\tilde{U}/\rho \to \infty$) which, for $\hbar\omega_0 = 0.8$ and $n = 0.7$, are given by 6.3 and 5.9, respectively. The lowering of the transition point may be explained by the correlation-induced carrier localization which increases with U and suppresses the double site-occupancy. Correspondingly, this localization effect supports the self-trapping localization of a single polaron which results in the decrease of the transition threshold. By the same reasonings, the increase of the effective polaron mass (decrease of ρ) below the transition with increasing U (see Fig. 3) may be understood. Let us emphasize that this behavior holds provided that $\tilde{U} > 0$ for all ε_p up to the transition to the heavy polaron state. For the MVLF without squeezing, this transition is nearly independent of n (cf. the chain dashed curves in Fig. 3a–c). This behavior must be interpreted as an effect of the exact two-dimensional density of states. Using the simple square density of states, for $U = 15$ (MVLF without squeezing) we obtain the transition points $\varepsilon_c(n)$: $\varepsilon_c(0.1) = 4.96$, $\varepsilon_c(0.5) = 5.40$, and $\varepsilon_c(0.7) = 5.84$. Obviously, with increasing electron density the kinetic energy contribution dominates the correlation energy (at fixed U), so that it becomes more difficult to localize the charge carriers.

In addition to this finite-density effect, the squeezing effect (increasing with n) also implies a shift of the self-trapping transition to higher values of ε_p (cf. the discussion in Sect. 3). That means, the squeezing effect counteracts the correlation effect (due to U), which is also demonstrated in Fig. 3. Considering Fig. 3b–c, the difference in ε_c, at $U = 15$, without and with squeezing is smaller for $n = 0.7$ than for $n = 0.5$. Moreover, the curves for $U = 15$ with squeezing belonging to $n = 0.5$ and $n = 0.7$ show coinciding transition points. From those results we see the counteracting tendencies of squeezing and correlation, where for certain parameter regions the squeezing effect may compensate the correlation effect.

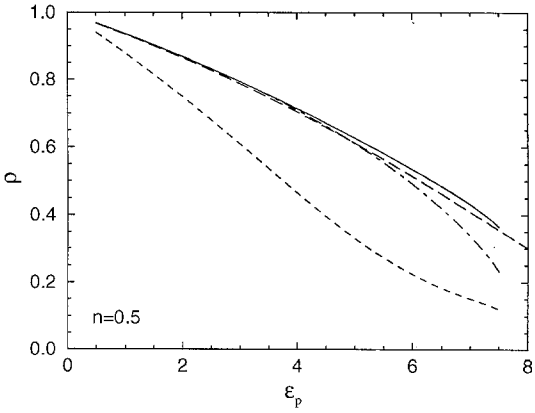

Fig. 4. Band narrowing factor ρ vs ε_p for $\hbar\omega_0 = 3.0$ and $n = 0.5$. The notations are the same as in Fig. 3

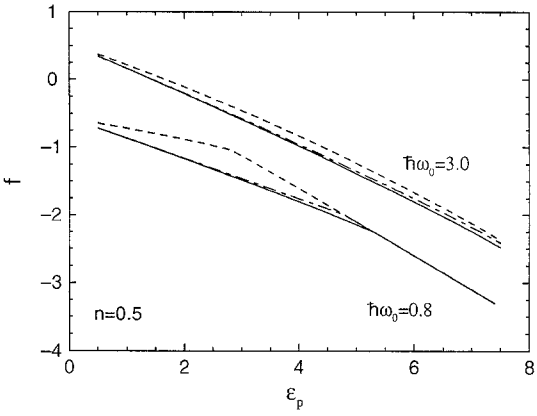

Fig. 5. Ground-state energy f in dependence on the polaron binding energy ε_p at $U = 15$, $n = 0.5$ for $\hbar\omega_0 = 0.8$ and 3.0. The MVLF solution with $\tau^2 \neq 1$ (solid line) is compared with the results, where both the MVLF (chain dashed) and the VLF (dashed) are used for $\tau^2 \equiv 1$

As seen in Fig. 3, the VLF yields a decrease of the transition point compared with the MVLF results (see also Fig. 2), where this deviation increases with the density.

In Fig. 4, the band narrowing factor is depicted for a frequency ($\hbar\omega_0 = 3.0$), for which the sharp self-trapping transition is suppressed. However, as for $\hbar\omega_0 = 0.8$, with increasing U the effective polaron mass is enhanced (where the correlation effect increases with n). Comparing Figs. 3 and 4, with increasing frequency the squeezing effect on the light-polaron mass is reversed: whereas for $\hbar\omega_0 = 0.8$, ρ below the transition point is decreased by squeezing (Fig. 3), for higher frequencies (Fig. 4) squeezing leads to an increase in ρ.

In Fig. 5 we have plotted the ground-state energies belonging to some of the solutions shown in Figs. 3 and 4. The self-trapping transition is reflected as a kink point in the energy curves. Furthermore, it can be seen explicitly that the solution in the MVLF has a lower energy than that in the VLF.

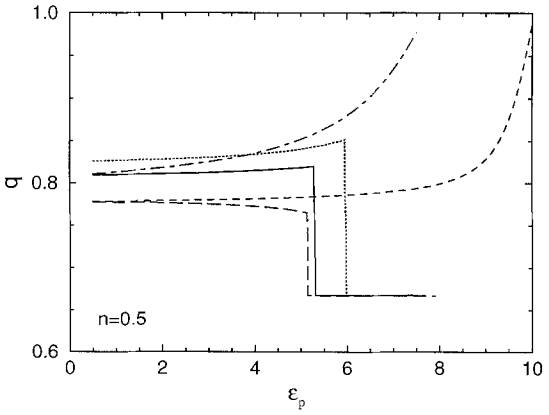

Fig. 6. Band narrowing factor q vs ε_p for the MVLF at $n=0.5$ with: $\hbar\omega_0=0.8$ and $U=15$ (solid), $U=20$ (long-dashed); $\hbar\omega_0=3.0$ and $U=15$ (chain dashed), $U=20$ (short-dashed). The dotted curve belongs to $\hbar\omega_0=0.8$, $U=15$, where the square density of states is used

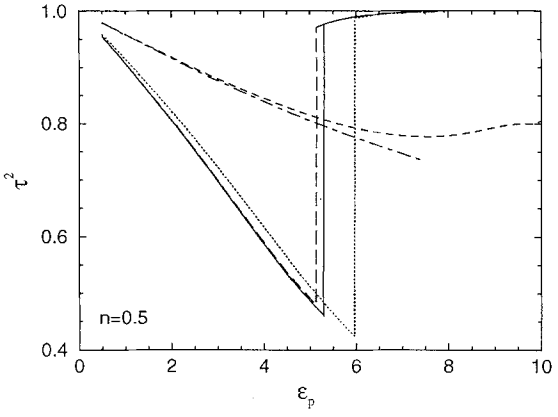

Fig. 7. Squeezing variational parameter τ^2 as function of the polaron binding energy ε_p. Parameters and notations are as in Fig. 6

In the presence of correlation, the effective polaron mass is determined by the band narrowing factor $q\rho$, where the correlation narrowing ($q<1$) and the polaron narrowing ($\rho<1$) are coupled (cf. the self-consistency scheme given by Eqs. (23)–(30)). As shown in Fig. 6, the factor q changes abruptly at the self-trapping transition from higher to lower values, in qualitative agreement with the behavior of ρ. With increasing correlation, q below the transition is reduced, as expected. Above the transition, the ratio $\tilde{U}/\rho$ is of the order of 10^3 to 10^4 provided that $\tilde{U}>0$. Therefore, q takes the value in the $\tilde{U}/\rho\to\infty$ limit given by (31). For higher frequencies ($\hbar\omega_0=3.0$), q continuously increases with ε_p and, of course, we have $q\to 1$ for $\tilde{U}\to 0$.

The dependence of the squeezing variational parameter τ^2 on ε_p is displayed in Fig. 7. For $\hbar\omega_0=0.8$, below the self-trapping transition, the effect of squeezing is to weaken the band narrowing forced by ε_p, i.e., the squeezing phenomenon increases with ε_p. In the heavy polaron region, squeezing becomes negligible due to the strong localization of the polarons. At high enough ω_0 (see the curves for $\hbar\omega_0=3.0$ in Fig. 7), τ^2 shows a smooth variation with ε_p. With increasing Coulomb interaction U, the squeezing effect is reduced which becomes more pronounced with increasing n. This again elucidates the counteracting effects of squeezing and correlation.

5. Polaron hopping conductivity

To investigate the finite-density and correlation effects on the polaron conductivity, we start from the polaronic Hamiltonian $\tilde{\mathscr{H}}$ (Eq. (5) with $\bar{\gamma}=(1-\gamma)n$). We confine ourselves to the heavy polaron regime ($\rho\ll 1$, see Fig. 1), where squeezing phenomena become negligible (cf. Sect. 4). That is, in (5) we take $\tau^2\equiv 1$ and denote $\tilde{\Phi}_{ij}(\tau^2\equiv 1)\equiv\Phi_{ij}$ given by (8).

The real part of the electrical conductivity is given by the Kubo formula

$$\mathrm{Re}\,\sigma(\omega)=\frac{\tanh(\beta\hbar\omega/2)}{2\Omega\hbar\omega}\int_{-\infty}^{\infty}\mathrm{d}t'\,\mathrm{e}^{i\omega t'}\langle[\tilde{J}^{\nu},\tilde{J}^{\nu}(t')]_+\rangle_{\tilde{\mathscr{H}}}. \quad (32)$$

Ω is the crystal volume, $\beta=1/k_BT$, and $\tilde{J}^{\nu}$ denotes the ν-component of the polaron current operator

$$\tilde{\mathbf{J}}=\frac{e}{i\hbar}\sum_i\mathbf{R}_i[\tilde{n}_i,\tilde{\mathscr{H}}]_-=\frac{iet}{\hbar}\sum_{\langle i,j\rangle\sigma}(\mathbf{R}_i-\mathbf{R}_j)\Phi_{ij}c_{i\sigma}^{\dagger}c_{j\sigma}, \quad (33)$$

where $\tilde{n}_i=n_i$. Since we are in the heavy polaron regime, we decouple the polaron-phonon correlation function appearing in the current correlator into a product of a dynamical polaron and phonon correlation function. Then, those functions are calculated, in the spirit of our variational approach, on the basis of $\tilde{\mathscr{H}}_0=\tilde{\mathscr{H}}_p+\tilde{\mathscr{H}}_e$ resulting from $\tilde{\mathscr{H}}$ by decoupling the phonon and polaron subsystems. Here, $\tilde{\mathscr{H}}_p=\hbar\omega_0\sum_i(b_i^{\dagger}b_i+\frac{1}{2})$, and $\tilde{\mathscr{H}}_e$ is given by (11) with the last term omitted and with ρt replaced by the polaronic reduced transfer integral

$$\tilde{t}=t\langle\Phi_{ij}\rangle_0=t\exp\{-\kappa\coth(\beta\hbar\omega_0/2)\},$$
$$\kappa=\frac{\varepsilon_p}{\hbar\omega_0}\gamma^2 \quad (34)$$

($\langle\ldots\rangle_0$ denotes the thermal average with respect to $\tilde{\mathscr{H}}_0$). Since we are primarily interested in the low-temperature conductivity, the variational parameter γ is taken from our ground-state analysis given in Sect. 4. Our main concern is the characteristics of the polaron-enhanced optical absorption by multiphonon processes in the low temperature regime. Therefore, we disregard the polaron band contribution and consider only the polaron hopping conductivity which is due to polaron transitions accompanied by multiphonon absorptions and emissions. The hopping contribution is given by

$$\langle\tilde{J}^{\nu}\tilde{J}^{\nu}(t')\rangle_0=-\left(\frac{et}{\hbar}\right)^2\sum_{\substack{\langle i,j\rangle\sigma\\ \langle l,m\rangle\sigma'}}(R_i^{\nu}-R_j^{\nu})(R_l^{\nu}-R_m^{\nu})$$
$$\cdot\langle c_{i\sigma}^{\dagger}c_{j\sigma}c_{l\sigma'}^{\dagger}(t')c_{m\sigma'}(t')\rangle_0$$
$$\cdot(\langle\Phi_{ij}\Phi_{lm}(t')\rangle_0-\langle\Phi_{ij}\rangle_0\langle\Phi_{lm}\rangle_0). \quad (35)$$

Since in the heavy polaron regime we have $\tilde{t} \ll \hbar\omega_0$, U, we calculate the hopping conductivity $\mathrm{Re}\{\sigma_h(\omega)\}$ to the lowest order in $\tilde{t}$, i.e. we take the polaron correlation function in the atomic limit of $\mathscr{H}_e$. We obtain

$$\langle c_{i\sigma}^{\dagger} c_{j\sigma} c_{l\sigma'}^{\dagger}(t') c_{m\sigma'}(t')\rangle_{\mathrm{a.l.}} = K_{ij}(t')\,\delta_{lj}\delta_{mi}\delta_{\sigma\sigma'}, \tag{36}$$

$$K_{ij}(t') = K_0 + K_1 \mathrm{e}^{\frac{i}{\hbar}\tilde{U}t'} + K_{-1}\mathrm{e}^{\frac{-i}{\hbar}\tilde{U}t'},$$

$$K_0 = \left(\frac{n}{2} - K\right)(1-n+2K),$$

$$K_1 = \left(\frac{n}{2} - K\right)^2, \qquad K_{-1} = \mathrm{e}^{-\beta\tilde{U}} K_1, \tag{37}$$

where

$$K \equiv \langle n_{i\uparrow} n_{i\downarrow}\rangle_{\mathrm{a.l.}} = \frac{n}{2} f(\tilde{U} - \tilde{\mu}). \tag{38}$$

Here $f(\varepsilon)$ is the Fermi function, and $\tilde{\mu} = \tilde{\varepsilon}_p + \mu$. By $\mathscr{H}_p$ we get the phonon correlation function

$$\langle \Phi_{ij}\Phi_{ji}(t')\rangle_0 = \langle \Phi_{ij}\rangle_0^2 \exp\{2\kappa[(p+1)\mathrm{e}^{i\omega_0 t'} + p\,\mathrm{e}^{-i\omega_0 t'}]\}, \tag{39}$$

where $p = 1/(\exp(\beta\hbar\omega_0) - 1)$.

Expanding the exponential we obtain

$$\langle \Phi_{ij}\Phi_{ji}(t')\rangle_0 - \langle \Phi_{ij}\rangle_0^2$$
$$= \langle \Phi_{ij}\rangle_0^2 \left\{ 2\sum_{s=1}^{\infty}\sum_{k=0}^{\infty} \frac{1}{(s+k)!\,k!}\left(\frac{\eta}{2}\right)^{s+2k} \cdot \cosh(s\beta\hbar\omega_0/2 + i s\omega_0 t') + \sum_{k=1}^{\infty}\frac{1}{(k!)^2}\left(\frac{\eta}{2}\right)^{2k}\right\}, \tag{40}$$

where $\eta = 2\kappa \sinh^{-1}(\beta\hbar\omega_0/2)$. Inserting Eqs. (35), (36), (40) into (32) we get

$$\mathrm{Re}\,\sigma_h(\omega) = 2\frac{N}{\Omega}\left(\frac{e a}{\hbar}\right)^2 \tilde{t}^2 \frac{\tanh(\beta\hbar\omega/2)}{\hbar\omega} \int_{-\infty}^{\infty} \mathrm{d}t'\,\mathrm{e}^{i\omega t'} \left\{ K_{ij}(t') \cdot \left[2\sum_{s=1}^{\infty} I_s(\eta)\cosh(s\beta\hbar\omega_0/2 + i s\omega_0 t') + I_0(\eta) - 1\right] + \mathrm{c.c.}\right\}, \tag{41}$$

where

$$I_s(\eta) = \sum_{k=0}^{\infty} \frac{1}{\Gamma(s+k+1)\,k!}\left(\frac{\eta}{2}\right)^{s+2k} \tag{42}$$

is the modified Bessel function. Taking $K_{ij}(t')$ from (37) and performing the time integration in (41) we obtain the optical absorption spectrum ($\omega > 0$)

$$\mathrm{Re}\,\sigma_h(\omega) = 8\pi\frac{N}{\Omega}\left(\frac{e a}{\hbar}\right)^2 \tilde{t}^2 \left\{ \sum_{s=1}^{\infty} I_s(\eta)\left[K_0 \frac{\sinh(s\beta\hbar\omega_0/2)}{s\hbar\omega_0}\,\delta(\omega - s\omega_0) + K_1\,\mathrm{e}^{-\beta\tilde{U}/2}\left(\frac{\sinh\left(\frac{\beta}{2}(\tilde{U} + s\hbar\omega_0)\right)}{\tilde{U} + s\hbar\omega_0}\,\delta\left(\omega - \frac{\tilde{U}}{\hbar} - s\omega_0\right) + \frac{\sinh\left(\frac{\beta}{2}(\tilde{U} - s\hbar\omega_0)\right)}{\tilde{U} - s\hbar\omega_0} \cdot \left(\delta\left(\omega - \frac{\tilde{U}}{\hbar} + s\omega_0\right) + \delta\left(\omega + \frac{\tilde{U}}{\hbar} - s\omega_0\right)\right)\right)\right] + K_1\,\mathrm{e}^{-\beta\tilde{U}/2}\frac{\sinh(\beta\tilde{U}/2)}{\tilde{U}}(I_0(\eta) - 1)\,\delta\left(\omega - \frac{\tilde{U}}{\hbar}\right)\right\}. \tag{43}$$

The δ-functions in (43) express the energy conservation in polaron transitions with or without changes in the number of doubly occupied sites accompanied by multiphonon emissions and absorptions. For example, the first term in (43) describes processes without changes in the number of doubly occupied sites and with the net emission of s phonons. The second term gives contributions from the creation of doubly occupied sites with the net emission of s phonons, whereas the change in the number of doubly occupied sites described by the last term is accompanied by an equal number of emitted and reabsorbed phonons.

Using the envelope of the δ-functions, Eq. (43) can be expressed as

$$\mathrm{Re}\,\sigma_h(\omega) = 8\pi\frac{N}{\Omega}\left(\frac{e a}{\hbar}\right)^2 \frac{\tilde{t}^2}{\omega_0}\left\{ \frac{\sinh(\beta\hbar\omega/2)}{\hbar\omega}\left[K_0 I_{\omega/\omega_0}(\eta) + K_1\,\mathrm{e}^{-\beta\tilde{U}/2} \cdot \left(I_{\left(\omega - \frac{\tilde{U}}{\hbar}\right)/\omega_0}(\eta) + I_{\left(\frac{\tilde{U}}{\hbar} - \omega\right)/\omega_0}(\eta) + I_{\left(\omega + \frac{\tilde{U}}{\hbar}\right)/\omega_0}(\eta)\right)\right] + K_1\,\mathrm{e}^{-\beta\tilde{U}/2}\frac{\sinh(\beta\tilde{U}/2)}{\tilde{U}}(I_0(\eta) - 1)\,\delta\left(\omega - \frac{\tilde{U}}{\hbar}\right)\right\}. \tag{44}$$

Note that $I_{\omega/\omega_0}(\eta)$ has meaning only for $\omega \geqq \omega_0$.

Let us now consider the low-temperature limit ($k_B T \ll \hbar\omega_0$, $\tilde{U}$) of the absorption spectrum in the case $n < 1$. Concerning the correlation functions (37), in the atomic limit we get $\lim_{T\to 0} \mathrm{e}^{(-\beta\tilde{\mu})} = 2(1-n)/n$ so that $K(T=0) = 0$ and

$$K_0(T=0) = \frac{n}{2}(1-n), \qquad K_1(T=0) = \frac{n^2}{4}. \tag{45}$$

The low-temperature expansion of (44) gives contributions to the zero-temperature spectrum only from the first two terms. Thus, we obtain

$$\mathrm{Re}\,\sigma_h(\omega; T=0) = 2\pi\frac{N}{\Omega}\left(\frac{e a}{\hbar}\right)^2 \frac{\tilde{t}^2}{\omega_0}\frac{1}{\hbar\omega}\left\{ n(1-n)\,B(\omega) + \frac{n^2}{2}\,B\left(\omega - \frac{\tilde{U}}{\hbar}\right)\right\}, \tag{46}$$

where

$$B(\omega) = (2\kappa)^{\frac{\omega}{\omega_0}}\,\Gamma^{-1}(1 + \omega/\omega_0); \qquad \omega \geqq \omega_0. \tag{47}$$

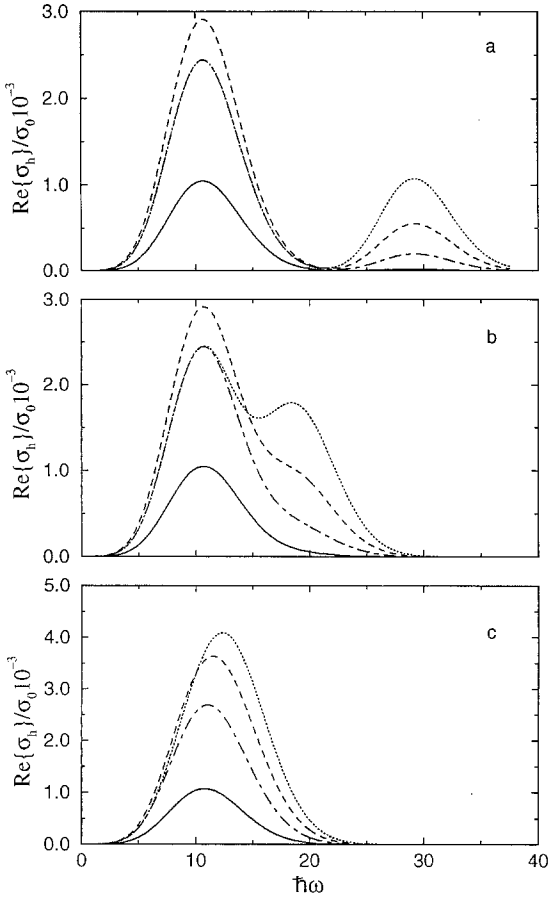

Fig. 8a–c. Real part of the hopping conductivity $\mathrm{Re}\{\sigma_h\}$ (in units of $\sigma_0 = 2\pi N e^2 a^2/\Omega\hbar$) as function of frequency at $\varepsilon_p = 6$ and $\hbar\omega_0 = 0.8$. The results are shown for $U = 30$ **a**, $U = 20$ **b** and $U = 15$ **c**, where full, chain dashed, dashed and dotted lines correspond to $n = 0.1$, $n = 0.3$, $n = 0.5$ and $n = 0.7$, respectively

Note that in the low-density limit $n \ll 1$ (first order in n) and in the $\tilde{U} = 0$ limit, the absorption spectra (44) and (46) agree with those obtained for uncorrelated polarons and for the LF by Loos [16]. In [16] the spectra are shown to reproduce the results by Reik (for $T = 0$ and $\omega \gg \omega_0$) and by Reik and Heese [14] (for not too low temperatures and $\varepsilon_p > \hbar\omega_0$).

We have numerically evaluated the zero-temperature absorption spectrum (46) for $\varepsilon_p = 6t$, $\hbar\omega_0 = 0.8t$ and for various sets of the parameters U and $n < 1$. That is, we consider the heavy polaron region, where multiphonon and nonadiabatic processes take place ($\hbar\omega_0 < t < \sqrt{\hbar\omega_0 \varepsilon_p}$ [17]). In addition, we take the Hubbard interaction U to be large enough so that $\tilde{U} \gg \tilde{t}$.

The absorption spectra are shown in Fig. 8. For $U = 30$ (Fig. 8a) we have $\gamma \simeq 1$ for all n (e.g. $n = 0.5$: $\gamma = 0.997$, $\rho = 6.2 \times 10^{-4}$). In this very heavy polaron region we compare our results with the LF ($\gamma \equiv 1$) spectrum given by Suzuki et al. [18]. We obtain a low-energy peak at $\hbar\omega_{m1} \simeq 2(\varepsilon_p - \hbar\omega_0)$ $\forall n$, in agreement with the position of the small-polaron maximum at about $2\varepsilon_p$ found in single-polaron theories (see, e.g., [4, 13, 16]). The peak position given in [18] ($\hbar\omega_{m1} \simeq \varepsilon_p$) is incorrect. For the peak width at half height we get $\Delta_1 = 7.3$ for all n, [18]: $\Delta_1 \simeq \sqrt{2\kappa}\hbar\omega_0 = 3.1$). The polaron correlation ($\tilde{U} = 18$) gives rise to a high-energy peak at $\hbar\omega_{m2} \simeq U - \hbar\omega_0$ [18]: $\hbar\omega_{m2} \simeq U - \varepsilon_p$) with the same width, where the peak height increases with n. Note that the low-energy absorption is symmetric with respect to $n = 0.5$.

In order to get more insight into the correlation effects on the optical absorption, in Fig. 8b, c the spectra are shown for $U = 20$ and $U = 15$, respectively. The variational parameter γ has nearly the same value as for $U = 30$, since $\tilde{U}/\rho$ is of the order of 10^4 in all cases. For $U = 20$ (15) we have $\tilde{U} = 8$ (3) $\forall n$. Owing to the decreasing value of $\tilde{U}$, the second contribution to (46) starts to merge with the first one so that the spectrum may show only one peak at $\hbar\omega_m$. Considering the case $U = 15$ (Fig. 8c), due to the increasing weight of the second contribution with increasing n, $\hbar\omega_m$ as well as the peak width increase with n. Thus, for not too strong polaron correlations and high enough densities it is possible to obtain a shift of the polaron absorption maximum to higher energies and a broadening of the spectrum. For fixed U, this correlation effect increases with n. On the other hand, for fixed n, the broadening of the single peak increases with $\tilde{U}$ and, for high enough values of $\tilde{U}$, a two-peak structure evolves (see Fig. 8a).

Let us relate this behavior to some recent attempts at interpreting the midinfrared absorption in high-T_c materials [11, 26] in terms of polaron hopping transport [11, 12, 18]. The photoinduced absorption spectra in the insulating phase of those compounds exhibit a maximum in the midinfrared which may be well fit by $\mathrm{Re}\{\sigma_h(\omega, T = 0)\}$ in the low-density limit [11] (where polaron interactions can be neglected). Considering, e.g., $YBa_2Cu_3O_{6.3}$, the peak position observed at 0.13 eV yields a polaron binding energy of $\varepsilon_p \simeq 0.07$ eV. In the metallic samples, where we have appreciable values of the charge carrier density, the conductivity maximum is reported to shift to lower energies with increasing carrier concentration [26], in disagreement with our polaron theory. In any case, the peak observed in the metallic samples is broader than calculated within single-polaron transport theory [11, 12]. This additional broadening (for $\omega > \omega_m$), also known from the small-polaron material TiO_2 [15], was recently suggested to be due to polaron correlations [11, 12] or to finite $\tilde{t}$ corrections to $\sigma_h(\omega)$ [18] (not included in (46)). As shown by our analysis, for appropriate parameter values, the broadening of the midinfrared peak may be due to polaron correlations. Let us point out that, besides the interpretation of the midinfrared absorption by polaron hopping, recently, strong arguments for explaining this absorption by Cu–O singlet to nonbonding oxygen transitions were given [27].

6. Conclusions

The main results of our variational approach to the polaron formation and of our hopping conductivity calculation in the Holstein-Hubbard model are the following.

(i) Below a critical phonon frequency, with increasing electron-phonon coupling ε_p a discontinuous transition

at ε_c from light polarons ($\rho \lesssim 1$) to self-trapped heavy polarons ($\rho \ll 1$) takes place. The critical coupling ε_c increases with frequency and is nearly equal to the half-bandwidth. For higher frequencies, there is a smooth crossover from light to heavy polarons. Qualitatively, the same behavior also holds for the spinless Holstein model.

(ii) The density effects on the polaron formation, treated by the modified variational Lang-Firsov transformation, are mainly realized via squeezing effects. With increasing density, the self-trapping transition is shifted to higher couplings. Using the (energetically unfavourable) variational Lang-Firsov transformation [17], the self-trapping transition is shifted to lower couplings.

(iii) Considering polaron correlations in the case of an effective Coulomb repulsion (treated by the slave-boson saddle-point approximation), with increasing Hubbard interaction the self-trapping transition is shifted to lower couplings, i.e. the correlation effect counteracts the squeezing effect. Below the transition, the effective polaron mass is enhanced by increasing correlation strengths.

(iv) The zero-temperature absorption spectra due to heavy-polaron hopping reveal qualitative finite-density and correlation effects. In addition to the low-energy maximum (known from single-polaron theories), the finite-density effects are particularly reflected in the correlation-induced high-energy structures.

(v) Depending on the model parameters, the interplay of the Hubbard interaction and the polaron density may give rise to a correlation-induced broadening of one effective absorption maximum. We conclude that this behavior may be relevant for the explanation of the anomalous midinfrared absorption in the metallic high-T_c materials.

Concerning the nature of the self-trapping transition, it is well known that a variational calculation can induce artifacts in the critical behavior. More elaborate approximations may rule out the discontinuous nature of this transition, but, in accord with Monte Carlo results [6], may yield a rather sharp transition from a quasi-free electron metal to a heavy-polaron metal. Accordingly, we conclude that our variational slave boson approach provides at least a qualitatively correct description.

Since the emphasis of this work was on the self-trapping of single polarons, we restricted ourselves to large values of the Hubbard interaction U so that the effective interaction $\tilde{U}$ is repulsive for all considered coupling strengths. In the case $\tilde{U} < 0$, the formation of bipolarons is possible, which may give rise to a bipolaronic superconducting ground state [9]. These problems will be left for further study.

H.F. and J.L. acknowledge the support of the NTZ and the hospitality at the University of Leipzig where part of this work has been performed.

References

1. Holstein, T.: Ann. Phys. **8**, 325 (1959); ibid. **8**, 343 (1959)
2. Toyozawa, Y.: Prog. Theor. Phys. **26**, 29 (1961). In: Kuper, C.G., Whitfield, G.D. (eds.) Polarons and excitons, p. 211. Edinburgh: Oliver and Boyd 1963
3. Sumi, A., Toyozawa, Y.: J. Phys. Soc. Jpn. **35**, 137 (1973)
4. Emin, D.: Adv. Phys. **12**, 57 (1973); ibid. **24**, 305 (1975)
5. Lang, I.G., Firsov, Y.A.: Zh. Eksp. Teor. Fiz. **43**, 1843 (1962); Firsov, Y.A.: Polarons. Moscow: Nauka 1975
6. Raedt, H.D., Lagendijk, A.: Phys. Rev. Lett. **49**, 1522 (1982); Phys. Rev. B**27**, 6097 (1983); ibid. **30**, 1671 (1984)
7. Klamt, A.: J. Phys. C**21**, 1953 (1988)
8. Lépine, Y., Gutiérrez, R.: Solid State Commun. **85**, 155 (1993)
9. Ranninger, J.: Z. Phys. B**84**, 167 (1991)
10. Kim, Y.H., Foster, C.M., Heeger, A.J., Cox, S., Stucky, G.: Phys. Rev. B**38**, 6478 (1988)
11. Mihailović, D., Foster, C.M., Voss, K., Heeger, A.J.: Phys. Rev. B**42**, 7989 (1990)
12. Bi, X.X., Eklund, P.C.: Phys. Rev. Lett. **70**, 2626 (1993)
13. Eagles, D.M.: Phys. Rev. **130**, 1381 (1963); ibid. **145**, 645 (1966)
14. Reik, H.G.: Z. Phys. **203**, 364 (1967); Reik, H.G., Heese, D.: J. Phys. Chem. Solids **28**, 581 (1967)
15. Kudinov, E.K., Mirlin, D.N., Firsov, Y.A.: Fiz. Tverd. Tela **11**, 2789 (1969)
16. Loos, J.: Z. Phys. B**71**, 161 (1988); Loos, J., Straka, J.: Czech. J. Phys. B**39**, 316 (1989)
17. Feinberg, D., Ciuchi, S., de Pasquale, F.: Int. J. Mod. Phys. B**4**, 1317 (1990)
18. Suzuki, Y.Y., Pincus, P., Heeger, A.J.: Phys. Rev. B**44**, 7127 (1991)
19. Trapper, U., Fehske, H., Deeg, M., Büttner, H.: Z. Phys. B**93**, 465 (1994)
20. Zheng, H.: Phys. Rev. B**37**, 7419 (1988); ibid. **38**, 11865 (1988); ibid. **41**, 4723 (1990)
21. Zheng, H., Feinberg, D., Avignon, M.: Phys. Rev. B**39**, 9405 (1989); ibid. **41**, 11557 (1990)
22. Fehske, H., Deeg, M., Büttner, H.: Phys. Rev. B**46**, 3713 (1992)
23. Deeg, M., Fehske, H., Büttner, H.: Z. Phys. B**88**, 283 (1992)
24. Kotliar, G., Ruckenstein, A.E.: Phys. Rev. Lett. **57**, 1362 (1986)
25. Frésard, R., Wölfle, P.: Int. J. Mod. Phys. B**5 & 6**, 685 (1992)
26. Uchida, S., Ido, T., Takagi, H., Arima, T., Tokura, Y., Tajima, S.: Phys. Rev. B**43**, 7942 (1991)
27. Wagner, J., Hanke, W., Scalapino, D.J.: Phys. Rev. B**43**, 10517 (1991)